

Growth and Characterization of Pure and Ni²⁺ Added Crystals of Glycinepotassiumsulfate

A. Karolin*, K. Jayakumari**, C. K. Mahadevan*

*Physics Research Centre, S.T.Hindu College, Nagercoil-629002, Tamilnadu, India.

**Department of Physics, SreeAyyappa College, Chunkankadai-629807, Tamilnadu, India.

ABSTRACT

Pure and Ni²⁺ added glycine potassium sulfate (GPS) single crystals were grown by the slow evaporation technique. Crystalline nature of the pure and doped crystals has been studied by XRD analysis. Fourier transform infrared (FTIR) studies confirm the functional group of the crystals. Their mechanical behavior has been assessed by Vickers microhardness measurements and nonlinear optical property has been tested by Kurtz and Perry powder technique. Thermal and dielectric studies were also carried out.

Keywords: Crystal growth, Dielectric crystal, Electrical properties, Mechanical properties, Optical properties, X-ray diffraction

I. Introduction

Alpha glycine (α -glycine) is the simplest amino acid which readily reacts with a majority of acids and salts forming an important group of electronic materials. New electronic materials of α -glycine can be synthesized from solutions containing specific ratios of the components. Ferroelectric property was reported for glycine silver nitrate [1], diglycine manganese chloride [2] and glycine phosphate [3]. Hoshino et al [4] reported about the dielectric properties of triglycinefluoroberyllate. Some complexes of α -glycine with inorganic salts have already been reported to be promising materials for SHG: glycine zinc chloride [5], glycine lithium chloride [6], glycine zinc sulfate [7], glycine sodium nitrate [8], etc. It was also reported that glycine combines with H₂SO₄ [9], CaCl₂ [10], CaNO₃ [11], BaCl₂ [12], SrCl₂ [13] and CoBr₂ [14]. These do not exhibit nonlinear optical (NLO) property.

Shanmugavadivu et al [15] grew glycine potassium sulfate (GPS) by mixing γ -glycine with potassium sulfate in equimolar ratio, which is a nonlinear optical (NLO) material too. They found that GPS crystal belongs to orthorhombic system with crystallographic parameters $a=5.7709\text{\AA}$, $b=7.4710\text{\AA}$, $c=10.0608\text{\AA}$, cell volume $V=433.7653\text{\AA}^3$ and space group P222. SHG efficiency of GPS was found to be higher than that of KDP. However, it would be better to improve the size and quality of the crystal.

In the present work, an attempt has been made to combine α -glycine instead of γ -glycine to grow better crystals of glycine potassium sulfate.

II. Experimental

2.1. Crystal growth

Glycine Potassium Sulfate (GPS) was synthesized from AR grade α -glycine and potassium

sulfate. The solubility study of pure GPS was carried out in a solvent of double distilled water at five different temperatures (30, 35, 40, 45, and 50°C). The solubility was determined by dissolving GPS salt in 100ml of double distilled water at a constant temperature with continuous stirring. After attaining the saturation, the equilibrium concentration of the solute was estimated gravimetrically. The variation of solubility with temperature is shown in Fig. 1. It can be seen that the solubility increases with the increase in temperature.

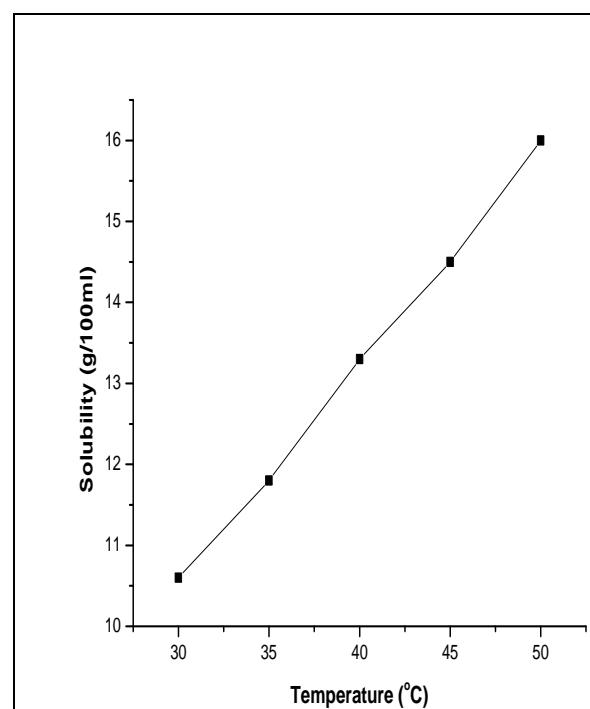
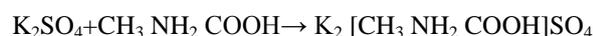


Figure 1: The solubility curve for pure GPS

An aqueous solution of GPS was prepared by dissolving α -glycine and potassium sulfate in the ratio 1:1 in double distilled water. The solution was filtered and kept in a dust free environment. Transparent and colorless single crystals of glycine potassium sulfate (GPS) were formed at room temperature in a period of about 25 days as per the reaction;



GPS was added with $NiSO_4 \cdot 7H_2O$ in five different molar ratios, viz. 1:0.002, 1:0.004, 1:0.006, 1:0.008 and 1:0.010 and the five different Ni^{2+} doped GPS crystals were grown in a period of about 25 days similarly under identical conditions with the pure GPS crystal growth.

2.2. Characterizations

Density was measured by the flotation method [16, 17] within an accuracy of $\pm 0.008 g/cm^3$. Carbon tetrachloride of density $1.594 g/cm^3$ and bromoform of density $2.890 g/cm^3$ were respectively the rarer and denser liquids used.

Atomic absorption spectroscopic (ASS) measurements were carried out using an atomic absorption analyzer (Model AA-6300) to determine the metal atom content of the impurity added crystals grown.

Single crystal X-ray diffraction (SXRD) analysis was performed and lattice parameters were determined for the pure and Ni^{2+} doped GPS crystals using a BRUKER KAPPA APEX II diffractometer with CuK_{α} radiation ($\lambda = 1.54056 \text{ \AA}$). X-ray powder diffraction (PXRD) analysis was carried out for all the six crystals grown using an automated X-ray powder diffractometer (PANalytical) in the 2θ range $10-70^\circ$ with CuK_{α} radiation ($\lambda = 1.54056 \text{ \AA}$). The reflection data were indexed following the procedures of Lipson and Steeple [18].

Fourier transform infrared (FTIR) spectra were recorded by the KBr pellet method for all the six crystals grown in the wavenumber range $400-4000 cm^{-1}$ by using a SHIMADZU spectrometer.

The UV-Vis-NIR absorption spectra were recorded in the wavelength range $190-1100 nm$ for all the six crystals grown by using a Lambda-35 spectrophotometer.

The NLO property of the grown crystals was tested by passing the output of Nd:YAG Quanta ray laser (with fundamental radiation of wavelength $1064 nm$) through the crystalline powder sample (Kurtz and Perry method [19]). The SHG output from the sample was compared with that from KDP.

Vickers hardness measurements were carried out on all the grown crystals by making indentations on the large area faces using a SHIMADZU HMV2 micro hardness tester.

A rough thermal test was conducted by heating the crystals up to $250^\circ C$ from room temperature. All the six crystals were found to be

thermally stable atleast up to $200^\circ C$. The capacitance (C_{crys}) and dielectric loss factor ($\tan \delta$) measurements were carried out to an accuracy of $\pm 2\%$ for all the six crystals grown by having the large area faces touching the electrodes by the conventional parallel plate capacitor method using an LCR meter (Agilent 4284A) at various temperatures ranging from $40-120^\circ C$ with five different frequencies, viz. $100 Hz, 1 kHz, 10 kHz, 100 kHz$ and $1 MHz$ in a way similar to that followed by Mahadevan and his co-workers [20-22]. The temperature was controlled to an accuracy of $\pm 1^\circ C$. The observations were made while cooling the sample. The dimensions of the crystal were measured using a traveling microscope. Air capacitance (C_{air}) was also measured. Since the variation of air capacitance with temperature was found to be negligible, air capacitance was measured only at the lower temperature considered. The crystals were shaped and polished and the opposite faces were coated with graphite to form a good conductive surface layer (ohmic contact). The sample was mounted between the silver electrodes and annealed at $120^\circ C$ for about 30 min to homogenize the sample before taking the readings.

As the crystal area was smaller than the plate area of the cell, the dielectric constant (ϵ_r) of the crystal was calculated using Mahadevan's formula [23-25]:

$$\epsilon_r = \left[\frac{A_{air}}{A_{crys}} \right] \left[\frac{C_{crys} - C_{air} \left(1 - \frac{A_{crys}}{A_{air}} \right)}{C_{air}} \right]$$

where C_{crys} is the capacitance with crystal (including air), C_{air} is the capacitance of air, A_{crys} is the area of the crystal touching the electrode and A_{air} is the area of the electrode. The ac conductivity (σ_{ac}) was calculated using the relation:

$$\sigma_{ac} = \epsilon_0 \epsilon_r \omega \tan \delta$$

where ϵ_0 is the permittivity of free space ($8.85 \times 10^{-12} C^2 N^{-1} m^{-2}$) and ω is the angular frequency ($\omega = 2\pi f$; $f = 100 Hz - 1 MHz$ in the present study).

III. Results and discussion

3.1. Densities, lattice parameters and chemical composition

The single crystals grown in the present study are represented as: Pure GPS \rightarrow the undoped GPS crystal; GP1, GP2, GP3, GP4 and GP5 \rightarrow 0.2, 0.4, 0.6, 0.8 and 1.0 mol% Ni^{2+} doped GPS crystals respectively.

Fig. 2 shows a photograph of the pure and Ni^{2+} added GPS single crystals grown in the present study. The grown crystals are transparent and colorless. Morphology of the Ni^{2+} doped GPS crystals is observed to be similar to that of the pure GPS crystal. Also, significant coloration did not occur due to Ni^{2+} doping.

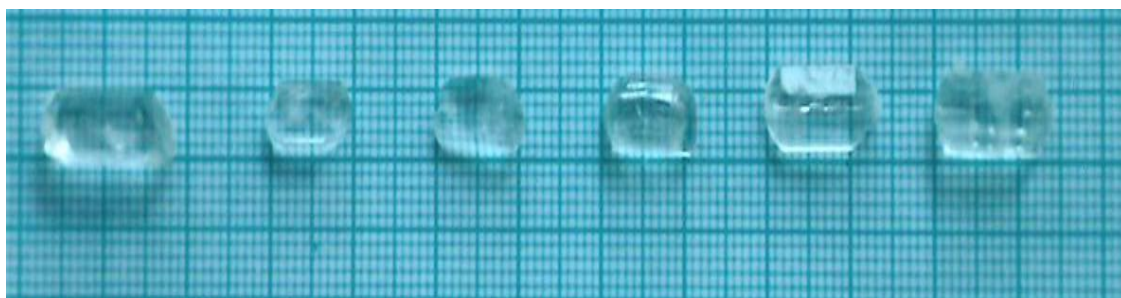


Figure 2: Photograph showing the pure and Ni²⁺ doped GPS crystals
 (From left: Pure GPS, GP1, GP2, GP3, GP4 and GP5)

The observed densities and Ni atom (dopant) contents (through AAS measurement) are given in Table 1. The observed Ni atom contents confirm the presence of Ni atom in the doped GPS crystals. The density decreases with the increase in impurity (dopant) concentration. This may be due to the incorporation of Ni atoms in the interstitial positions and/or due to the replacement of K atoms by the Ni atoms in the host (GPS) crystal matrix. Results obtained through density and AAS measurements indicate clearly that the dopant atoms have entered proportionately with the GPS crystal matrix nearly as per the dopant concentration considered in the solution used for the growth of single crystals.

Unit cell parameters obtained from single crystal X-ray diffraction analysis for the pure and Ni²⁺ doped GPS crystals are given in Table 1. Pure and Ni²⁺ doped GPS crystals belong to orthorhombic system with space group Pmcn. The lattice parameters obtained for pure GPS (grown in the present study using α -glycine) agree well with those obtained for GPS crystal grown using γ -glycine [15]. However, it is found that α -glycine leads the crystal system to become centrosymmetric.

The observed difference in the lattice volumes is very small to have any lattice distortion in the GPS crystal due to doping. This confirms that the dopant atoms have entered into the GPS crystal matrix but not distorted the regular structure of the GPS crystal. In addition the lattice volume does not vary systematically with the dopant concentration indicating the dopant concentrations considered in the present study are significantly small to create any lattice distortion in the GPS crystal.

The recorded PXRD patterns of the grown crystals are shown in Fig.3. Appearance of sharp and strong peaks confirms the crystalline nature of the samples. The diffraction peaks were indexed for the orthorhombic system.

The FTIR spectra of pure and doped GPS crystals are shown in Fig.4. Significant difference could not be observed for the doped crystals due to the lower level of dopant concentration. The transmission due to the carboxylate group of free glycine is normally observed in the region 607 and 1413cm⁻¹, whereas in the case of GPS, these peaks are shifted to 619.11 and 1400.22cm⁻¹,

Table 1: Densities, Ni atom contents and lattice parameters for the pure and Ni²⁺ doped GPS crystals. The e.s.d.s are in parenthesis.

Crystal	Density (g/cm ³)	Ni content (ppm)	Lattice parameters			
			a (Å)	b (Å)	c (Å)	Volume(Å ³)
Pure GPS	2.562	-	5.7503 (1)	7.4520 (1)	10.0275 (2)	429.6 (1)
GP1	2.487	81	5.7436 (2)	7.4526 (2)	10.0980 (3)	432.2 (3)
GP2	2.475	85	5.7900 (2)	7.5300 (4)	10.0210 (3)	436.9 (1)
GP3	2.469	100	5.7339 (1)	7.4890 (4)	10.0321 (4)	431.2 (2)
GP4	2.452	134	5.7850 (2)	7.5231 (2)	10.0440 (1)	437.1 (2)
GP5	2.428	152	5.7410 (1)	7.4270 (3)	10.0301 (2)	427.7 (1)

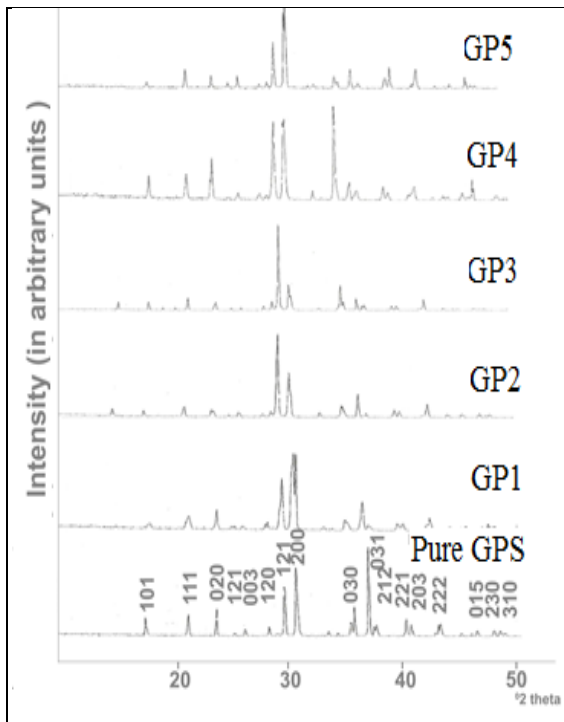


Figure 3: The powder X-ray diffraction patterns for pure and Ni²⁺ added GPS crystals

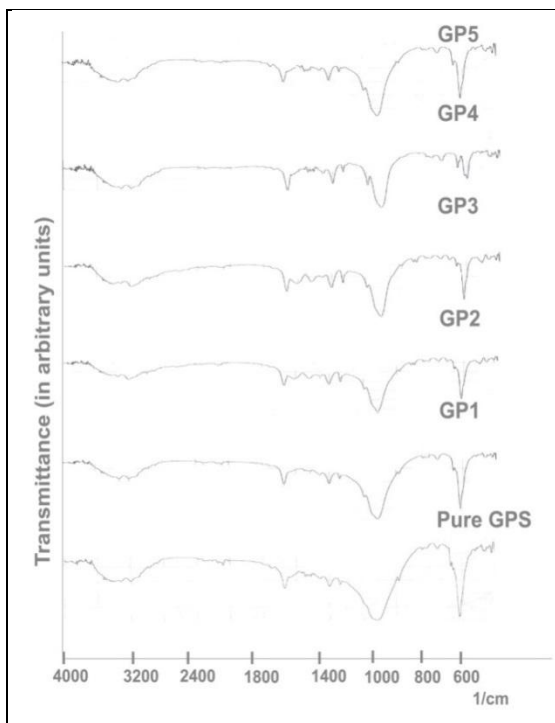


Figure 4: The FTIR spectra for pure and Ni²⁺ doped GPS crystals

respectively. Similarly, the transmission peaks for the NH₃⁺ group of free glycine are observed at 1110, 1507 and 3175cm⁻¹ respectively. In the GPS crystal, NH₃⁺ groups of free glycine are shifted to 1116.7, 1512.09 and 3197.75cm⁻¹. This observation confirms that glycine exists in the zwitterionic form and the involvement of NH₃⁺ in hydrogen bonding is evident

by the fine structure of the bond in the lower energy region (assignment given in Table 2). The peak at 981.7cm⁻¹ is due to CH₂ stretching vibration. Thus, with the help of available data on the vibrational frequencies of amino acids[26], all the molecular groups present in the GSS crystals could be identified.

3.2 UV – Vis – NIR spectral analysis

Fig.5 shows the UV – Vis – NIR optical absorption spectra of pure and Ni²⁺ doped GPS crystals. The cut off wavelengths lie below 300nm. It is found that the cut off wavelength is nearly equal for all crystals. The optical transparency of the GPS crystal is increased by the addition of impurity.

3.3 SHG measurements

From the experiment, it is noticed that there is no green light emitted from the sample and this gives the conclusion that the grown pure and Ni²⁺ doped GPS crystal gives zero second order susceptibility coefficient. This result is consistent with the observation of centro-symmetric space group (Pmcn) through X-ray diffraction studies.

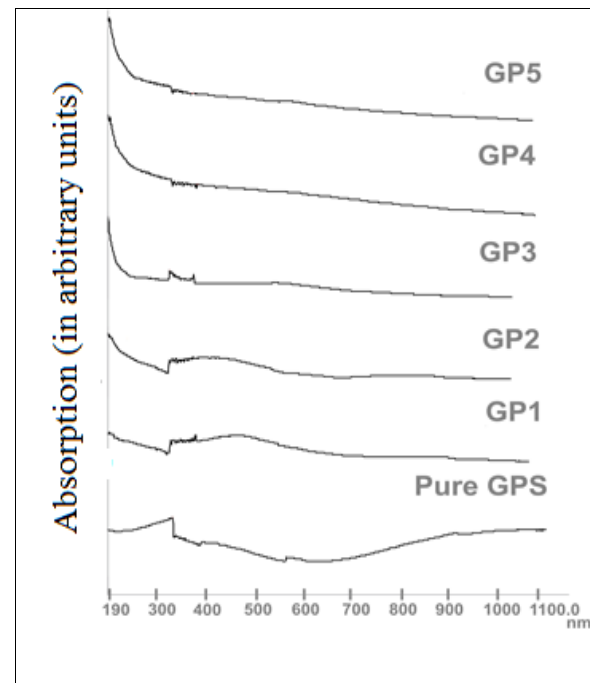


Figure 5: UV-Vis-NIR spectra for the pure and Ni²⁺ doped GPS crystals

3.4 Mechanical Properties

Hardness of a material is a measure of the resistance that materials present to local deformation and it is an important mechanical property of the optical materials for fabrication of devices. It can be used as a suitable measure for the strength of a material.

The plots of Vickers micro hardness number as a function of the applied load are shown in Fig.6. It is observed that the Vickers hardness number

increases with increasing load. Above 100g, cracks developed on the surface of the crystals due to the

release of internal stresses generated by indentation. Addition of Ni²⁺ ion is found

Table 2: Observed FTIR wavenumbers and their vibrational assignments for pure and Ni²⁺ added GPS crystals

Pure GPS	FTIR wavenumbers (cm ⁻¹) for					Assignments*
	Ni ²⁺ doped GPS					
	GP1	GP2	GP3	GP4	GP5	
3197	3197	3193	3193	3197	3197	$\gamma_{asy}\text{-NH}_3^+$
2084	2084	2115	2086	—	—	Combination bond
1674	1670	1668	1670	1670	1672	NH ₃ ⁺ deformation
1512	1512	1512	1523	1512	1527	NH ₃ ⁺ bending
1456	1454	1456	1456	1461	1456	γCH_2
1400	1400	1402	1402	1400	1400	$\gamma_{sy}\text{COO}^-$
1336	1336	1334	1334	1336	1336	CH ₂ wagging
1116	1116	1116	1114	1122	1118	NH ₃ ⁺ rocking, $\gamma_{sy}\text{SO}_4^{2-}$
981	981	—	981	—	—	γCH_2
744	748	746	746	750	748	SO ₄ ²⁻ bending
619	617	617	617	601	617	γSO_4^{2-}
520	—	503	505	516	518	COO ⁻ rocking

* γ . stretching vibration, γ_{asy} —asymmetric stretching vibration, γ_{sy} —symmetric stretching vibration

to increase the hardness value. Fig. 7 shows the plots of log d against log P for the pure and Ni²⁺ doped GPS crystals. The work hardening exponents were calculated from the slopes of the straight lines. The work hardening coefficients are found to be 3.49, 2.94, 3.23, 3.32, 3.23 and 2.6 respectively for pure and Ni²⁺ doped (GP1, GP2, GP3, GP4 and GP5) GPS crystals. Since the value of n is greater than 1.6, the grown crystals belong to soft material category [27].

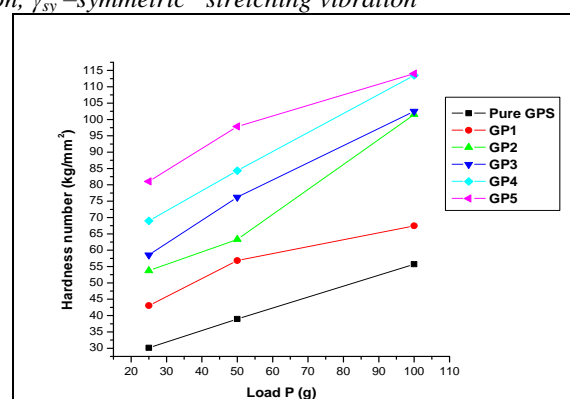


Figure6: Hardness behavior of pure and Ni²⁺ doped GPS crystals

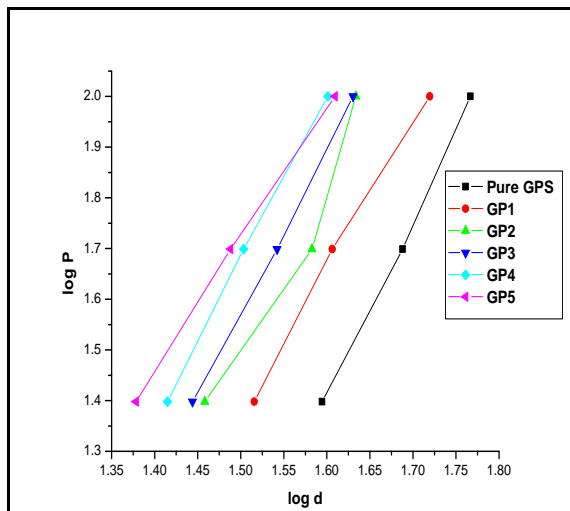


Figure7: The plots of log d versus log P for pure and Ni²⁺ doped GPS crystals

3.5 Dielectric properties

Figs.8-10 show the dielectric constants (ϵ_r), dielectric loss factors ($\tan\delta$) and AC conductivities (σ_{ac}) observed for the pure and Ni²⁺ doped GPS crystals. It can be seen that all the three dielectric parameters increase with the increase in temperature. The ϵ_r and $\tan\delta$ values decrease whereas the σ_{ac} value increases with increase in frequency. This indicates that all the six crystals grown in the present study exhibit normal dielectric behavior in the temperature and frequency ranges considered. Also, it is observed that the dielectric parameters do not vary systematically with the impurity concentration. The $\tan\delta$ values observed in the present study are considerably low which indicates that the crystals grown are of high quality.

The high dielectric constant at low frequency is due to the presence of all types of polarizations, viz. electronic, ionic, orientation, space charge, etc. The space charge polarization will depend on the purity and perfection of the sample. Its influence is large at high temperature and is not noticeable in the low frequency region. In normal dielectric behavior, the dielectric constant decreases with increasing frequency and reaches a constant value, depending on the fact that beyond a certain frequency of the electric field, the dipole does not follow the alternating field. The crystals with high dielectric constant lead to power dissipation. The material having low dielectric constant will have less number of dipoles per unit volume. As a result it will have minimum losses as compared to the material having high dielectric constant. Therefore the grown crystals may be used for high speed electro-optic modulations.

Variation of dielectric constant with temperature is generally attributed to the crystal expansion, the electronic and ionic polarizations and the presence of impurities and crystal defects. The variation at low temperature is mainly due to the crystal expansion and electronic and ionic

polarizations. The variation at high temperature is mainly due to the thermally generated charge carriers and impurity dipoles. Varotsos [28] has shown that out of the contribution from electronic and ionic polarizations, the electronic polarizability practically remains constant. The increase of dielectric constant with the increase of temperature is essentially due to the temperature variation of ionic polarizability. Thus the major contribution to the observed dielectric constant of the crystals grown in the present study can be from electronic and ionic polarizations.

Electrical conductivity of GPS crystals may be determined by the proton transport within the framework of hydrogen bonds. Conductivity mechanism in ice containing the hydrogen bonds and the conductivity associated with the incorporation of impurities into the crystal lattice can be combined to understand the conductivity mechanism in pure and impurity added crystals. The proton conduction can be accounted for by motion of protons accompanied by an excess of positive charge (D defects). Electric polarization may be modified by migration of these defects. However, migration of these defects may not change the charge at an electrode [29].

The motion of defects occurs by some kind of rotation in the bond with defects. When the temperature of the crystal is increased, there is a possibility of weakening of the hydrogen bonding system due to rotation of the carboxyl ions in the glycine molecules. The increase of conductivity with the increase of temperature observed for the pure and Ni²⁺ added GPS crystals in the present study can be understood as due to the temperature dependence of the proton transport.

For the pure and Ni²⁺ doped GPS crystals the observed σ_{ac} values were fitted to the Arrhenius relation:

$$\sigma_{ac} = \sigma_{0AC} \exp(-E_{ac}/kT)$$

Values of $\ln\sigma_{ac}$ were plotted against $(1000/T)$ for both the pure and Ni²⁺ doped GPS crystals (Fig. 11). AC activation energies were calculated from the slopes of the straight lines best fitted by least squares analysis. The estimated AC activation energies are provided in Table 3.

The low AC activation energies observed suggest that oxygen vacancies may be responsible for conduction in the temperature region considered in the present study.

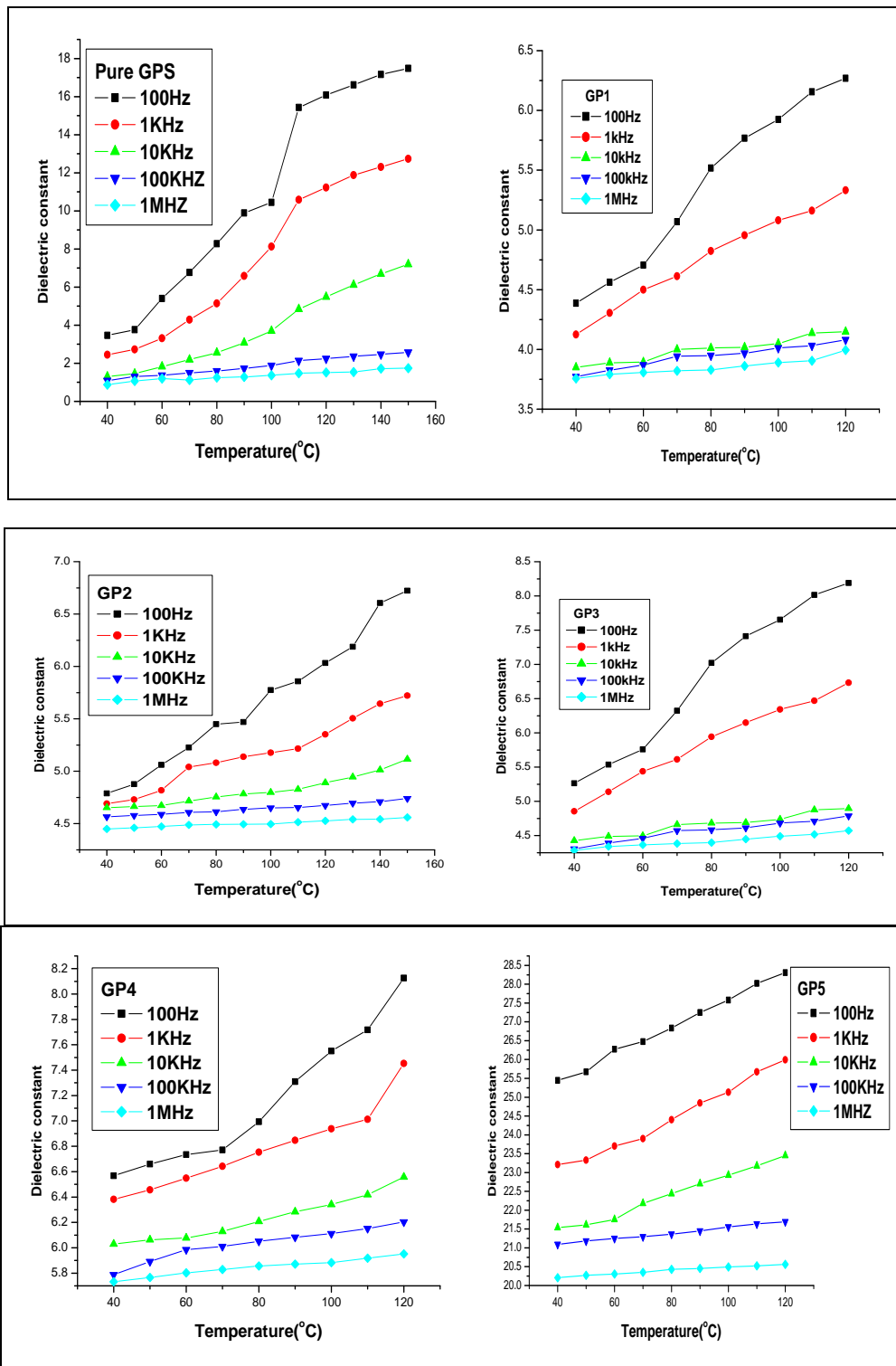


Figure 8: The dielectric constant (ϵ_r) values for the pure and Ni²⁺ doped GPS crystals

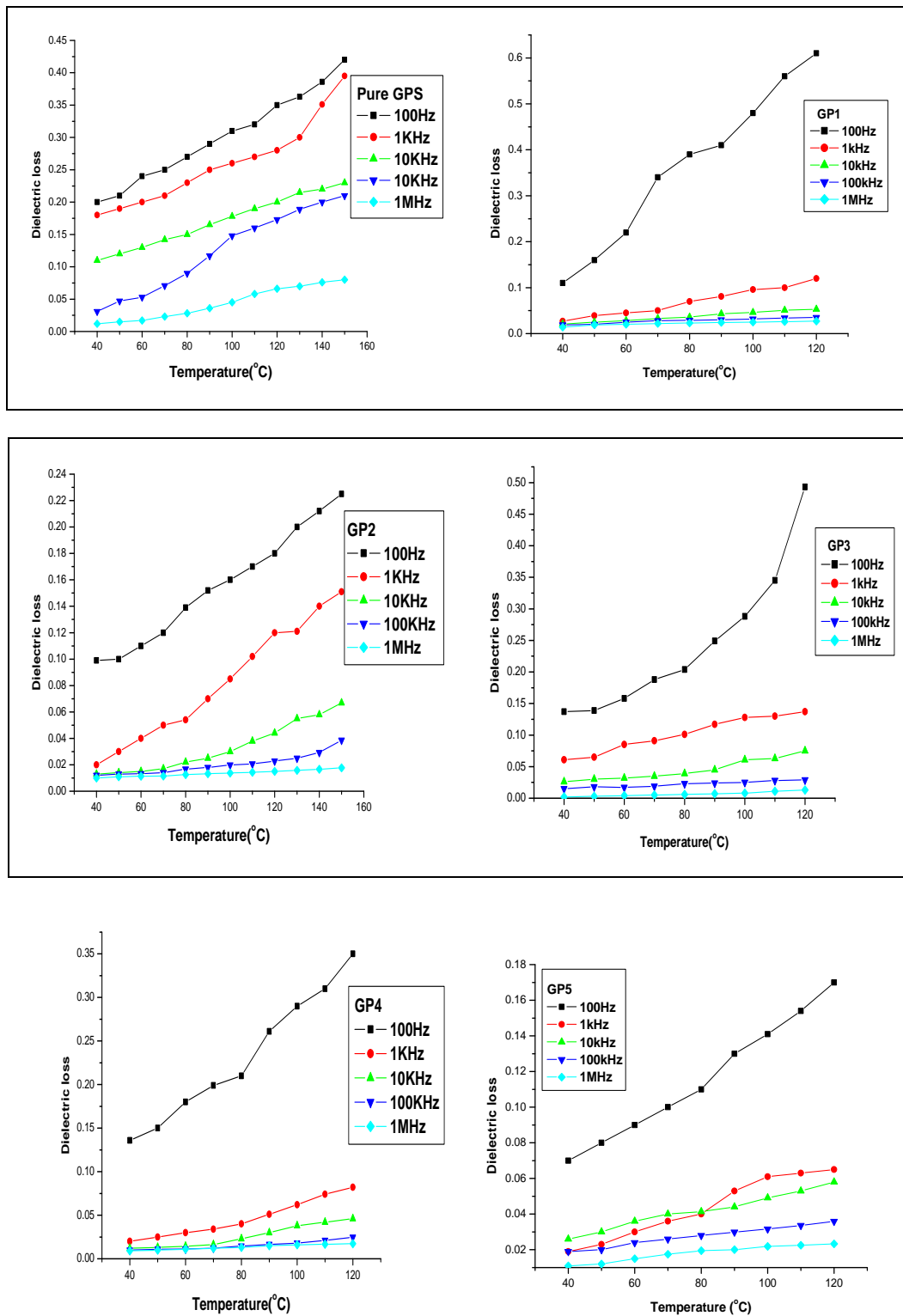


Figure 9: The dielectric loss factors ($\tan \delta$) for the pure and Ni^{2+} doped GPS crystals

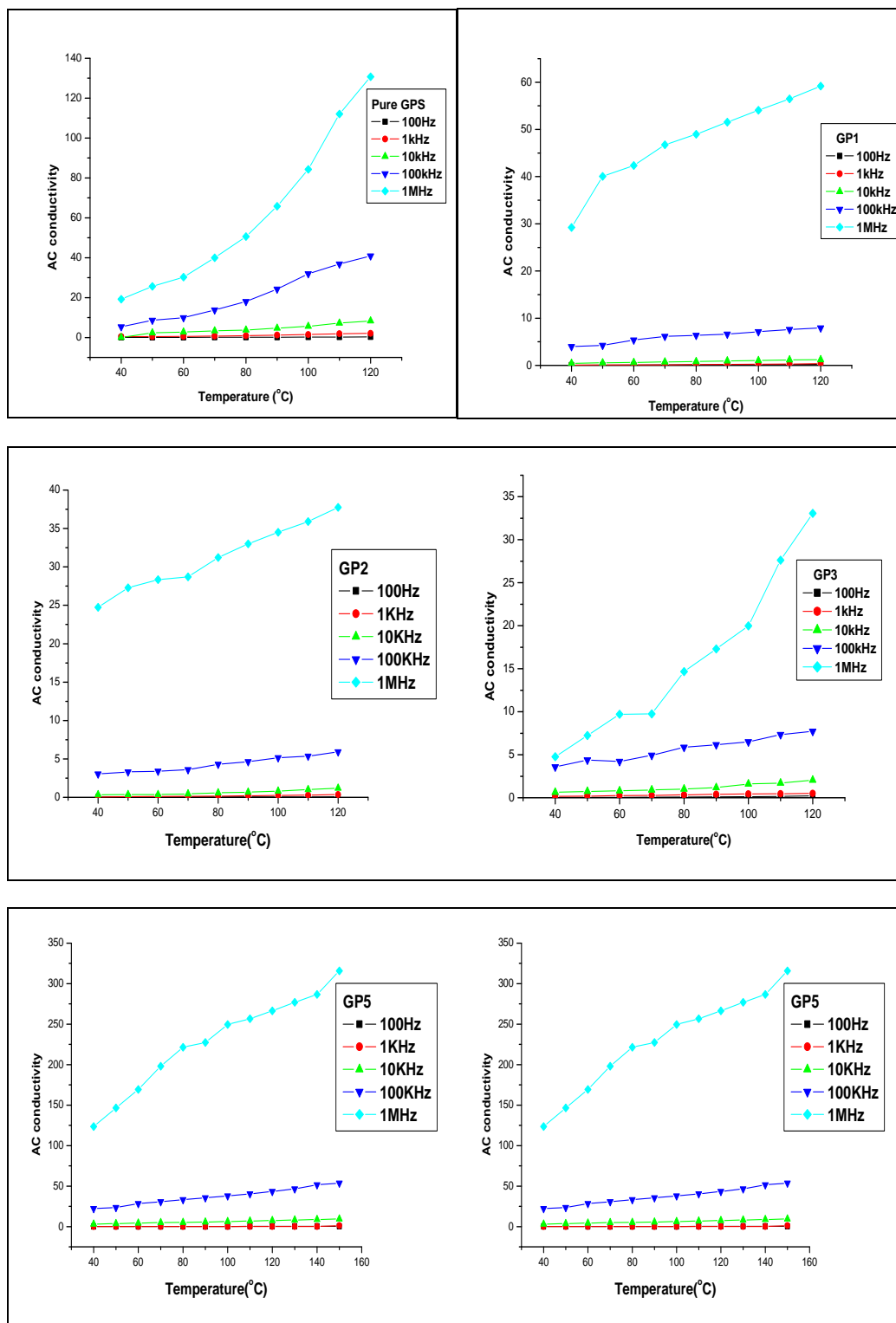


Figure 10: The AC electrical conductivities (σ_{ac}) ($\times 10^{-7}$ mho/m) for the pure and Ni^{2+} doped GPS crystals

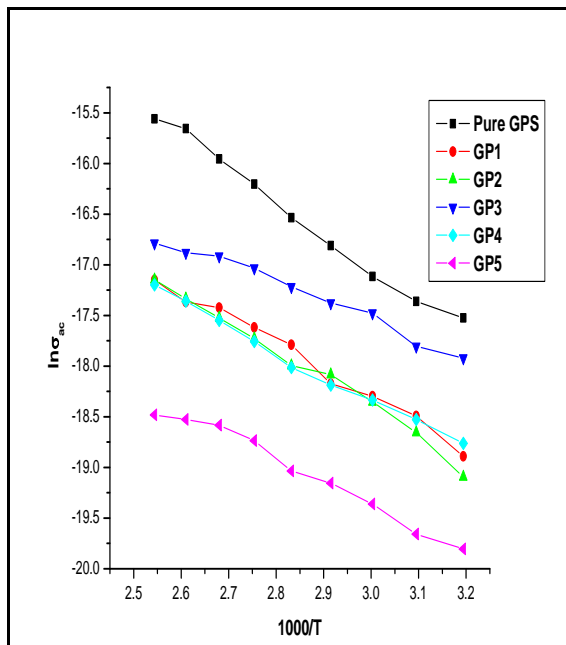


Figure 11: Variation of $\ln\sigma_{ac}$ with $1000/T$ (K^{-1}) for the pure and Ni^{2+} doped (GP1, GP2, GP3, GP4 and GP5) GPS single crystals

Table3: AC activation energies for the pure and Ni^{2+} doped GPS crystals

Crystal	Activation energy (eV)
Pure GPS	0.281
GP1	0.225
GP2	0.245
GP3	0.157
GP4	0.208
GP5	0.190

IV. Conclusion

Pure and Ni^{2+} doped α -glycine potassium sulfate (GPS) single crystals have been successfully grown by the free evaporation method and characterized. X-ray diffraction measurements indicate no lattice distortion due to Ni^{2+} doping. The GPS crystal is found to be thermally stable at least up to $200^{\circ}C$ and mechanically soft. Tuning the optical, mechanical and electrical properties could be understood as possible by Ni^{2+} doping. All the six crystals grown are found to exhibit normal dielectric behavior. Analysis of the AC electrical conductivity data indicates that the conductivity in pure and Ni^{2+} doped GPS crystals is due to the proton transport.

References

[1] R. Pepinsky, Y.Okaya, D.P. Eastman, and T. Mitsui, *Phys. Rev.*, 107, 1957, 1538.
 [2] R. Pepinsky, K. Vedam and Y. Okaya, *Phys. Rev.*, 110, 1958, 1309.
 [3] A. Deepthy and H.L. Bhat, *J. Cryst. Growth*, 226, 2001, 287.

[4] S. Hoshino, T. Mitsui, F.Jona and R. Pepinsky, *Phys. Rev.*, 107, 1957, 1255.
 [5] T. Balakrishnan and K. Ramamurthi, *Mater. Lett.* 62, 2008, 65.
 [6] M. Lenin, G. Bhavannarayana and P. Ramasamy, *Opt. Commun.*, 282, 2009, 1202.
 [7] T. Balakrishnan and K. Ramamurthi, *Spectrochim. Acta Part A*, 68, 2007, 360.
 [8] J.H. Paredes, D.G. Mitnik, O.H. Negrete, H.E. Ponce, M.E. Alvarez R, R.R. Mijangos and A.D. Moller, *J. Phys. Chem. Solids*, 69, 2008, 1974.
 [9] S. Hoshino, Y. Okaya and R. Pepinsky, *Phys. Rev.* 115, 1959, 323.
 [10] S. Natarajan and J.K. Mohan Rao, *Z. Kristallogr.*, 152, 1984, 179.
 [11] S. Natarajan, K. Ravikumar and S.S. Rajan, *Z. Kristallogr.*, 168, 1984, 75.
 [12] P. Narayanan and S. Venkataraman, *Z. Kristallogr.*, 142, 1975, 52.
 [13] K. Ravikumar and S.S. Rajan, *Z. Kristallogr.* 171, 1985, 201.
 [14] J. Baran, M. Drozd, A. Pietraszko, M. Trzebiatowska and H. Ratajczak, *J. Polym. Chem.*, 77, 2003, 1561.
 [15] Ra. Shanmugavadu, G. Ravi and A. Nixon Azariah, *J. Phys. Chem. Solids*, 67, 2006, 1858.
 [16] T.H. Freeda and C.K. Mahadevan, *Bull. Mater. Sci.*, 23, 2000, 335.
 [17] K. Jayakumari and C.K. Mahadevan, *J. Phys. Chem. Solids*, 66, 2005, 1705.
 [18] H. Lipson and H. Steeple, *Interpretation of X-ray power Diffraction Patterns*, MacMillan, New York, 1970.
 [19] S.K. Kurtz and T.T. Perry, *J. Appl. Crystallography*, 9, 1968, 3798.
 [20] S. Perumal and C.K. Mahadevan, *Physica B*, 367, 2005, 172.
 [21] G. Selvarajan and C.K. Mahadevan, *J. Mater. Sci.*, 41, 2006, 8218.
 [22] C.M. Padma and C.K. Mahadevan, *Mater. Manuf. Processes*, 23, 2007, 144.
 [23] M. Meena and C.K. Mahadevan, *Cryst. Res. Technol.*, 43, 2008, 166.
 [24] C.M. Padma and C.K. Mahadevan, *Physica B*, 403, 2008, 1708.
 [25] M. Priya and C.K. Mahadevan, *Cryst. Res. Technol.*, 44, 2008, 92.
 [26] R.S. Krishnan, K. Sankaranarayanan and K. Krishnan, *J. Indian Inst. Sci.*, 55, 1973, 313.
 [27] E.M. Onitsch, *Mikroskopie* 2, 1941, 135.
 [28] P.A. Varotsos, *J. De. Phys. Lett.* 39, 1978, L-79.
 [29] H. Granicher, C. Jaccard, P. Scherrer and A. Steinemann, *Discuss. Farad. Soc.* 23 (1957) 50.